HHS Public Access

Author manuscript

Hum Brain Mapp. Author manuscript; available in PMC 2017 December 01.

Published in final edited form as:

Hum Brain Mapp. 2016 December ; 37(12): 4673–4688. doi:10.1002/hbm.23336.

Heterochronicity of White Matter Development and Aging Explains Regional Patient Control Differences in Schizophrenia

Peter Kochunov[*,1], **Habib Ganjgahi**[*,2], **Anderson Winkler**[3], **Sinead Kelly**[4], **Dinesh Shukla**[1], **Xiaoming Du**[1], **Neda Jahanshad**[4], **Laura Rowland**[1], **Hemalatha Sampath**[1], **Binish Patel**[1], **Patricio O'Donnell**[5], **Zhiyong Xie**[5], **Sara A. Paciga**[6], **Christian R. Schubert**[6,7], **Jian Chen**[8], **Guohao Zhang**[8], **Paul M. Thompson**[4], **Thomas E. Nichols**[2,#], and **L. Elliot Hong**[1,#]

[1]Maryland Psychiatric Research Center, Department of Psychiatry, University of Maryland School of Medicine, Baltimore

[2]Department of Statistics, University of Warwick, Warwick, UK

[3]FMRIB Centre, Oxford University, Oxford, UK

[4]Imaging Genetics Center, Keck School of Medicine of USC, Marina del Rey, CA, USA

[5]Neuroscience Research Unit, Worldwide Research and Development, Pfizer Inc., 610 Main Street, Cambridge, MA 02139, USA

[6]Enterprise Scientific Technology Operations, Worldwide Research and Development, Pfizer Inc., Eastern Point Rd, Groton, CT 06340, USA

[7]Biogen, Cambridge, MA 02142, USA

[8]Department of Computer Science, University of Maryland, Baltimore County, MD 21228, USA

Abstract

Background—Altered brain connectivity is implicated in the development and clinical burden of schizophrenia. Relative to matched controls, schizophrenia patients show (1) a global and regional reduction in the integrity of the brain's white matter (WM), assessed using diffusion tensor imaging (DTI) fractional anisotropy (FA), and (2) accelerated age-related decline in FA values. In the largest mega-analysis to date, we tested if differences in the trajectories of WM tract development influenced patient-control differences in FA. We also assessed if specific tracts showed exacerbated decline with aging.

Methods—Three cohorts of schizophrenia patients (total n=177) and controls (total n=249; age=18–61 years) were ascertained with three 3T Siemens MRI scanners. Whole-brain and regional FA values were extracted using ENIGMA-DTI protocols. Statistics were evaluated using mega- and meta-analyses to detect effects of diagnosis and age-by-diagnosis interactions.

[*]Corresponding Author: (pkochunov@mprc.umaryland.edu), Address: Maryland Psychiatric Research Center, Department of Psychiatry, University of Maryland School of Medicine, Baltimore, MD, USA, Phone: (410) 402-6110, Fax (410) 502-6778.
[*]KP and GH share first authorship
[#]NTE and LEH share last authorship

Conflict of Interest

Authors declare no conflict of interest.

Results—In mega-analysis of whole-brain averaged FA, schizophrenia patients had lower FA (p=10^{-11}) and faster age-related decline in FA (p=0.02) compared to controls. Tract-specific heterochronicity measures, i.e., abnormal rates of adolescent maturation and aging explained ~50% of the regional variance effects of diagnosis and age-by-diagnosis interaction in patients. Interactive, 3D visualization of the results is available at www.enigma-viewer.org.

Conclusion—WM tracts that mature later in life appeared more sensitive to the pathophysiology of schizophrenia and were more susceptible to faster age-related decline in FA values.

Introduction

The genetic and environmental risk factors for schizophrenia may disproportionately affect brain areas with prolonged maturation, while sparing brain areas that develop soon after birth (Kochunov and Hong 2014). Cerebral white matter (WM) may especially be at risk of abnormal development, as many fiber tracts continue to develop into mid-adulthood, well past the average age of onset of schizophrenia (Flechsig 1901; Kochunov and Hong 2014; Yakovlev and Lecours 1967). The development of WM tracts is “heterochronic”: difference in timing of development and senescence among white matter regions. For example, motor and sensory white matter bundles become fully myelinated soon after birth (Gao, et al. 2009; Yakovlev and Lecours 1967) while multimodal associative fibers continue to develop into the 4th decade of life (Figure 1) (Bartzokis 2004; Bartzokis, et al. 2010; Flechsig 1901; Kochunov, et al. 2010a; Kochunov, et al. 2011a; Yakovlev and Lecours 1967). Age-related decline shows a reverse trend: multimodal associative fibers decline rapidly with age despite reaching peak myelination later in life (Bartzokis 2004; Bartzokis, et al. 2003; Flechsig 1901; Yakovlev and Lecours 1967). We hypothesized that WM areas that develop past the age of onset of schizophrenia and into adulthood will show larger patient-control differences as development past the age of onset will make them more vulnerable to schizophrenia risk factors and the disease itself. Second, we hypothesized that age-related decline would be accelerated in WM areas that develop later in life. The second hypothesis is based on the findings that later myelinated areas such as frontal WM are more vulnerable to chronic age-related illnesses such as hypertension, heart disorders and neurodegenerative disorders (Bartzokis 2004; Bartzokis, et al. 2003; Kochunov, et al. 2010b; Kochunov, et al. 2011b). Schizophrenia may increase individual risks for accelerated aging(Ito and Barnes 2009; Jeste, et al. 2011; Kirkpatrick, et al. 2008) due to increased rate of diseases commonly associated with aging including cardiovascular disease, type-2-diabetes and other (Hennekens, et al. 2005). Schizophrenia patients have increased mortality rate and shorter (by as much as twenty years) average lifespan even after accounting for suicide (Brown 1997; Kirkpatrick, et al. 2008; Saha, et al. 2007; Tsuang and Woolson 1978). We tested these hypotheses by mapping patient-control differences and accelerated WM aging in patients using diffusion tensor imaging (DTI) fractional anisotropy (FA) values. We measured patient-control DTI-FA differences and related them to previously published normative rates of cross-sectional regional DTI-FA maturation and decline calculated from a large group (N=831) of healthy individuals ages ranged from 11 to 90 that had no overlap with the present sample (Kochunov, et al. 2011a) (Table 1, Figure S1, see supplement).

WM integrity's rise during development is followed by a peak and age-related decline. WM development and aging trends are regionally heterochronic and some development continues into the 4th decade (Flechsig 1901; Kochunov, et al. 2012b; Yakovlev and Lecours 1967) (Figure 1) (Ben Bashat, et al. 2005; Flechsig 1901; Gao, et al. 2009; Kochunov, et al. 2011a; Kochunov, et al. 2012b). These regional differences in timing of development and aging in healthy populations have been mapped non-invasively using DTI-FA values (Hasan, et al. 2009a; Hasan, et al. 2009b; Kochunov, et al. 2012b). FA describes the directional selectivity of the random diffusion of water molecules (Basser 1994; Conturo, et al. 1996; Pierpaoli and Basser 1996; Ulug, et al. 1995). Higher FA values are observed in heavily myelinated WM tracts (Pierpaoli and Basser 1996), but absolute WM FA values are sensitive to myelination levels, the degree of intra-voxel fiber crossing, axonal density and average axonal diameter (Beaulieu 2002; Jones, et al. 2013). Changes in regional FA values during normal maturation, aging and brain disorders are often attributed changes in myelination (Budde, et al. 2007; Madler, et al. 2008; Song, et al. 2003; Song, et al. 2005). Nonetheless, the DTI-FA is neither a direct measurement of myelination nor of white matter integrity (Jones, et al. 2013). Instead, FA is a convenient index sensitive to the anisotropy of the water diffusion, created by intra-axonal flow and the barriers of cellular membranes, especially the myelin layer of the axonal cell membranes (Pierpaoli and Basser 1996).

Reduced fractional anisotropy (FA) emerged as a highly consistent finding in schizophrenia (Alba-Ferrara and de Erausquin 2013; Ellison-Wright and Bullmore 2009; Friedman, et al. 2008; Glahn, et al. 2013; Kubicki, et al. 2007; Nazeri, et al. 2012; Perez-Iglesias, et al. 2011; Phillips, et al. 2012; Wright, et al. 2015). Additional evidence to support our hypothesis includes reports that findings of lower FA values are more commonly observed in multimodal WM areas such as the frontal WM including the genu of corpus callosum versus motor and sensory areas (Ellison-Wright and Bullmore 2009; Friedman, et al. 2008; Kubicki, et al. 2007; Nazeri, et al. 2012; Perez-Iglesias, et al. 2011), even in young and unmedicated patients (Bloemen, et al. 2010; Carletti, et al. 2012; Karlsgodt, et al. 2009). Likewise there is evidence for accelerated decline in FA values in patients in multimodal WM areas including associative fibers in the corpus callosum (Friedman, et al. 2008; Kochunov, et al. 2014a; Kochunov, et al. 2012a; Mori, et al. 2007), a finding not observed in major depression (Kochunov, et al. 2012a). A challenge for testing this hypothesis is the need for a large sample to calculate the pattern of schizophrenia-related regional differences in FA, making it necessary to combine imaging data collected on multiple scanners. We used a mega-analysis approach developed by the ENIGMA-DTI workgroup (Jahanshad, et al. 2013b) to pool data from three independent cohorts. Besides the differences in imaging scanners, the overall ascertainment, clinical assessments, and control group recruitment used the same clinical methods across the three cohorts.

The mega-analysis developed by the ENIGMA-DTI working group uses data homogenization to create a single aggregated population by combining data across all cohorts. We previously used it to aggregate data across multiple cohorts (van Erp, et al. 2015); the mega-analytic estimates of brain differences were able to independently predict findings in later studies (Kochunov, et al. 2015a; Kochunov, et al. 2015b). We performed traditional meta-analysis by aggregating statistics from each separate cohort, which may be viewed as a more conservative approach. For each hypothesis test, we compared the

performance of the mega-analysis to that of the meta-analysis. We tested whether findings were consistent across three cohorts analyzed independently.

Methods

Subjects

We tested the study's hypotheses in three cohorts of subjects. All data were acquired at the Maryland Psychiatric Research Center (MPRC) over the last decade (2004–2015), each with its own healthy control group. The cohorts reflect the evolution of the imaging technology (cohort A is the most recent; cohort C was the first collected). No subject was included in more than one of the three cohorts. If a participant was initially in more than one cohort, only the latest scan was used. Uniform clinical assessment and exclusion criteria were equivalent across the three cohorts. Informed written consents, approved by the local Internal Review Boards, were obtained from all participants.

All participants were 18 to 61 years old, with no current or past neurological conditions or major medical conditions. Patient participants were diagnosed with either schizophrenia or schizoaffective disorder as determined by the Structured Clinical Interview for DSM-IV or IV-TR (SCID). Controls had no past or present Axis I psychiatric disorder as determined with the SCID. Participants were excluded if they had DSM-IV substance abuse in the last 3 months (except nicotine) or substance dependence within the past 6 months. Other exclusion criteria included diagnosis with uncontrolled hypertension, type 2 diabetes, heart disorders, or a major neurological event such as stroke or transient ischemic attack. All patients undergone a uniform psychiatric interview that included Brief Psychiatric Rating Scale (BPRS) assessment of clinical symptoms. Only current medication dose was recorded. The current medication use was converted to chlorpromazine equivalence. The data analyzed by this manuscript was collected under three research protocols. Here, we presented only the data that was available for all subjects across the protocols.

Cohort A

Subjects: This cohort included 205 participants (105/101 males/females, average age=35.3±13.6 years, range=18–61) (Table 2). Among them were 65 patients diagnosed with schizophrenia (44/21 males/females, age=34.6±13.7 years) and 140 healthy controls (61/79 males/females, age 35.6±13.8 years). Additional clinical and epidemiological information is provided in Table 2.

Diffusion tensor MR imaging: Imaging data was collected using a Siemens 3T TRIO MRI (Erlangen, Germany), running VB17 software and equipped with a 32-channel RF head coil. DTI data was collected using a spin-echo, EPI sequence with a spatial resolution of 1.7×1.7×3.0 mm. The sequence parameters were: TE/TR=87/8000 ms, FOV=200 mm, axial slice orientation with 50 slices and no gaps, 64 isotropically distributed diffusion weighted directions, two diffusion weighting values (b=0 and 700 s/mm^2) and five b=0 images. Subjects' head movement was minimized with restraining padding.

Cohort B

Subjects: Cohort B included a total of 113 (61/52 males/females, average age=38.5±11.3 years, range=18–61) individuals (Table 2). Among them 49 (33/16 males/females, age=35.3±9.5 years) were patients and 64 (27/37 males/females, age 40.3.0±11.9 years) were healthy controls (Table 2). Additional clinical and epidemiological information is provided in Table 2.

Diffusion tensor MR imaging: Imaging data was collected using a Siemens 3T TRIO MRI (Erlangen, Germany), running VB13 software and equipped with a 12-channel RF head coil. DTI data was collected using a spin-echo, EPI sequence with a spatial resolution of 1.8×1.8×3.0 mm. Sequence parameters were: TE/TR=92/6700 ms, FOV=210 mm, axial slice orientation with 49 slices and no gaps, 30 isotropically distributed diffusion weighted directions, two diffusion weighting values (b=0 and 1000 s/mm^2) and three b=0 values. Head movement was minimized with restraining padding.

Cohort C

Subjects: Cohort C included a total of 108 individuals (77/31 males/females, average age=38.3±13.0 years, range=18–61; Table 2). Among them were 63 patients (50/13 males/females, age=37.7±12.5 years), and 45 (27/18 males/females, age 39.1±13.8 years) were healthy controls (Table 2). Controls were recruited through media advertisements. Additional clinical and epidemiological information is provided in Table 2.

Diffusion tensor MR imaging: Imaging data was collected using a Siemens 3T Allegra MRI (Erlangen, Germany) running VA19 software and using a spin-echo, EPI sequence with a spatial resolution of 1.7×1.7×4.0 mm. The sequence parameters were: TE/TR=87/5000 ms, FOV=200 mm, axial slice orientation with 35 slices and no gaps, twelve isotropically distributed diffusion weighted directions, and two diffusion weighting values (b=0 and 1000 s/mm^2). The entire protocol was repeated five times to improve signal-to-noise ratio. Head movement was minimized with restraining padding and an individually fitted bite-bar. DTI data from this cohort has been used in a prior study of accelerated aging (Kochunov, et al. 2012a). We re-examined the mega-analysis results with and without this cohort and global and regional age-by-diagnosis interactions remained consistent.

Image processing

DTI data for all three cohorts was processed using the ENIGMA-DTI analysis pipeline (http://enigma.ini.usc.edu/ongoing/dti-working-group/), which includes quality control and assurance QC/QA steps (Jahanshad, et al. 2013b). Briefly, the DTI data were corrected for motion and eddy current distortions using the eddy correction tool distributed as a part of FMRIB Software Library (FSL) package (Smith, et al. 2006). FA maps were generated by voxel-wise fitting of the local diffusion tensor. Next, individual FA maps were warped to an ENIGMA-DTI template and projected onto the ENIGMA-DTI skeleton that represents the middle of the tract of major white matter structures. ENIGMA-DTI per-tract average values were calculated by averaging values along tract regions of interest in both hemispheres. Overall average FA values were calculated by averaging values for the entire white matter skeleton, including the tract regions of interest and also more peripheral white matter. DTI

data is sensitive to artifacts brought about by subject's motion(Yendiki, et al. 2014). All data included in the analysis passed the ENIGMA-DTI QA/QC. The QA/QC steps included: visual inspection of raw and FA images, followed by calculating the average subject motion per frame and the average projection distance onto the skeleton. Seven individual datasets, four from cohort A and three from cohort B, were removed from the analysis. Four datasets (two each from cohorts A and B) were removed as they exceeded the recommended threshold of 2.5 mm for the average motion per DTI frame (Acheson et al., In Review). There was no significant difference in the head motion between patient and controls in each cohort (p=0.6, 0.4 and 0.7 for cohorts A, B and C). Three data sets, from cohort B, were removed due to poor spatial normalization quality, with an average projection distance > 3.7mm (Acheson et al., In Review). There was no significant difference in the projection distance patient and controls in each sample (all p>0.5).

Statistical analyses

The two hypotheses were tested first using the mega and then using meta-statistical analyses. The first set of analyses quantified patient-control differences in FA values across different WM areas. The second set of analyses examined age-related decline in FA values. In both analyses, the patient-control differences and the age-related declines were compared to the normal rate of FA changes in different WM areas. The mega-analysis normalizes data from each cohort to remove scanner-and-cohort related biases in FA values (Table S1, see supplement) and then pools all the data together (Kochunov, et al. 2014c). We used the mega-analysis, developed by ENIGMA-DTI workgroup (Jahanshad, et al. 2013a; Kochunov, et al. 2014c) and implemented in the SOLAR-Eclipse software (http://www.nitrc.org/projects/se_linux). A classical meta-analysis was performed as a validation to demonstrate agreement between mega- and meta-analytical approaches of pooling data. We also repeated analyses in the three cohorts separately to examine if large biases arose from any particular cohort.

The significance of regional findings was corrected for multiple (N=12) comparisons using Bonferroni correction. Findings with $0.0042<p\leq0.05$ were deemed suggestively significant.

All significance testing was performed assuming two-tailed distribution. The significance of regional findings was corrected for multiple (N=12) comparisons using Bonferroni correction. Findings with $0.0042<p\leq0.05$ were deemed suggestively significant.

Patient-control FA differences

Mega-Analysis: The ENIGMA-DTI mega-analysis algorithm was used to combine the data into a single population following regression of nuisance covariates and data homogenization (Kochunov, et al. 2014c) (Figure S2, see supplement). The ENIGMA-DTI mega-analysis uses two normalization steps: regression of covariates, per cohort, followed by the per-cohort inverse Gaussian normalization of data (Figure S2-II, see supplement). This produced the mega-analytic sample for testing the model described in Equation 1:

$$FA=A+\beta_{DX}+\beta_{DX\times Age} \quad \text{(Eq 1)}$$

where age, sex, age^2, age×sex, age^{2}xsex were treated as cohort-specific covariates.

An example of this analysis is shown in Figure 2. The average FA values follow a nonlinear trend with age. Mega-analysis removes the quadratic age effects and thus producing linear patient-control differences in the aging trend (Figure 2). The linear DX x Age model (Eq1) may not account for non-linear aging differences between patients and controls. Therefore, we repeated DX x Age analyses in subjects older than the age-of-peak for the respective track. This analysis had different number of subjects for each track. This approach captures the mostly linear down-slope of the aging-related decline to re-assess the Dx x age effect. The goal of this ad-hoc analysis was to study consistency between $\beta_{DX\times Age}$ coefficients obtained using this approach and these obtained using the full sample.

Individual Cohort Analyses: The DX and DX×Age modeling in individual cohorts was also performed as a part of the meta analyses in each cohort independently (Figure S2-II, *bottom panel*)

$$FA=A+\beta_{DX}+\beta_{DX\times Age}+\beta_{Sex}+\beta_{Age}+\beta_{Age}{}^2+\beta_{Sex\times Age}+\beta_{Sex\times Age}{}^2 \quad \text{(Eq 2)}$$

The results were then used for the meta-analytical calculation of the overall effect (Figure S2-II, *bottom panel*). The cohort-specific modeling was performed using the R software using the lm function and maximum likelihood algorithm (R-Development-Core-Team 2009).

Meta-Analysis: The significance of the β_{DX} for each individual cohort was converted to Z-score statistics (Figure S2-II, *bottom panel*). The meta-analytical significance was calculated from the Z_{Meta} values obtained using the square-root of N-weighted Stouffer method (Stouffer 1949), (Equation 3):

$$Z_{Meta}=\frac{\sum_{i=1}^{3}\sqrt{N_i}\cdot Z_i}{\sqrt{\sum_{i=1}^{3}N_i}} \quad (3)$$

where Z_i and N_i are the z-value and sample size for cohort "i". The Stouffer meta-analysis method assigns greater weight to larger cohorts. It is reduced to the arithmetic mean of Z-values per cohort when the sample sizes are all equal.

Effects of symptom-severity, medication dosage and smoking on FA values— Post-hoc exploratory analyses were performed within the patients only to estimate effects of symptom severity and medication dose in the mega-analytic sample and for each cohort separately. Symptom severity was expressed as BPRS scores (coefficient β_{BPRS}), and medication dose at the time of the imaging expressed as milligram chlorpromazine equivalents calculated using the method described elsewhere(van Erp, et al. 2015) (CPZ;

coefficient β_{CPZ}). Models included nuisance effects as above. The statistical effects of smoking on FA values were analyzed in the mega-sample population and each cohort separately with a binary variable (SMK) 1 for smoker, 0 for non-smoker, including nuisance effects mentioned above.

Results

Effect of diagnosis on the global and regional FA values

Significant β_{DX} was observed during mega-analytic modeling of the effect of diagnosis on average FA ($p=1.3\times10^{-13}$), as well as in all three cohorts analyzed separately. The meta-analysis results showed similar significance ($p=1.1\times10^{-11}$) (Table 3). Interactive, 3D visualization of the results is available at www.enigma-viewer.org.

Regional mega-analytic β_{DX} coefficients were significantly correlated with both the rate of normal FA development (r=0.83, R^2=68.4%, p=0.001) and the rate of normal FA decline (r= 0.76, R^2=58.0%), p=0.005), the correlation with age of peak for FA values was positive but not statistically significant (r=0.35, p=0.2) (Figure 2).

Effect of age-by-diagnoses interaction on the global and regional FA values

The mega-analysis showed a significant age-by-diagnoses interaction for global FA (p=0.02), which suggested accelerated decline in FA values in patients compared with controls (Table 4). Meta-analysis showed a similar result (p=0.04). Similar trends in β_{Age*DX} effects were observed in all three cohorts separately (marginally significant in cohorts A and C (p= 0.04 for average FA) but not in cohort B (p=0.3) (Figure 3, Table 4). Significant (after correcting for multiple comparisons) mega-analytic $\beta_{Age\times DX}$ coefficients were observed for the genu and body of corpus callosum and corona radiata tract. No significant mega-analytic age-by-diagnosis interactions were observed for the following areas: internal capsule, superior longitudinal fasciculus, posterior thalamic radiation, and inferior and superior longitudinal fasciculi (Table 4). The regional contrast between the mega-analytical age-by-diagnoses trends are shown for genu of corpus callosum and posterior thalamic radiation (Figure S3). Following the removal of age and age^2 covariates, the normal controls and patients show diverging trends with age.

Regional mega-analytic $\beta_{Age\times DX}$ coefficients, were significantly correlated with both the rate of normal FA development and the rate of normal FA decline (r=0.69, R^2=49.0% and 0.80, R^2=64.0% p<0.05, respectively) in WM regions. The correlation with age of peak for FA values was positive but not statistically significant (r=0.46, p=.09) (Figure 3, *bottom row*).

The regional mega-analytic $\beta_{Age\times DX}$ coefficients recalculated in subjects older than the age-of-peak for respective tracts were highly correlated with the $\beta_{Age\times DX}$ coefficients obtained the full sample (r=0.84, p=0.0006) (Table S2, Figure S4, see supplement). However, the overall significance of the age-by-diagnosis interaction was reduced due to smaller number of subjects e.g. less than half of the subjects (N=229) were older than age-of-peak of 34 years for the genu of corpus callosum (Table S4, see supplement). The mega-analytic estimates of accelerated aging calculated past the age-of-peak for each area were

significantly correlated with the rates of normal development (r=0.70, R^2=0.49 p=0.015) and decline (r=0.69, R^2=0.48, p=0.016) and the age of peak (r=0.73, R^2=0.53, p=0.01) (Figure S5, see supplement)

Effects of symptom-severity, age-of-onset, disorder duration, medication dosage and smoking on FA values

We detected no significant effects of symptom severity, expressed as BPRS scores, on the FA values in patients for any of the three cohorts. There were no significant effects of age-of-onset and disorder duration on FA values following the regression of linear and quadratic effects of the age. There were no significant effects of medication dosage on the patients' FA values at the time of imaging (Table S3). Likewise, no significant effect of smoking was detected.

Comparisons between regional mega- vs. meta-analytic estimates

We performed a linear regression analysis to statistically compare effect sizes calculated using mega-analytic data pooling to that of the classical meta-analytic approach. Calculated effect sizes for diagnosis and age-by-diagnosis interaction were in excellent agreement (r>0.96) with mega-analytic estimates showing slightly (~5%) improved significance (lower p-values).

We repeated the mega-analysis of patient-control differences and aging trends by excluding subjects from cohort C who had been analyzed in our previous work to show accelerated aging in schizophrenia patients (Kochunov, et al. 2012a). Mega-analytic estimates for cohorts A and B showed excellent agreement (r>0.9) with the mega-analytic estimates in all three cohorts (Figure S6, **see** supplement), suggesting that the patient-control and accelerated aging trends were in good agreement among cohorts.

Discussion

In this largest schizophrenia DTI analysis to date, we observed regional variations in the level of patient-control FA deficits and accelerated decline of FA values in cerebral white matter (WM) with age in patients. These effects may results from the heterochronicity – or differential timing – of normal maturation and aging of cerebral WM. FA deficits in patients are more typically reported in WM tracts associated with higher cognitive function rather than in those that carry primary motor and sensory information (Lagopoulos, et al. 2013; Voineskos, et al. 2010; Wheeler and Voineskos 2014). This pattern was robustly (r^2~0.5) explained by known differences in the normal FA development rates across WM tracts. The direction of association indicates that the WM tracts that continued development to adulthood beyond the typical age of onset of schizophrenia had more prominent patient-control differences. Tracts with accelerated age-related decline in patients were also those that normally have steeper age-related decline. These tracts have prolonged maturation that goes beyond the typical age of onset of schizophrenia. The prolonged development of these tracts may expose them to the genetic and environmental risk factors for schizophrenia. These same risk factors may further contribute to their accelerated decline with age.

We found robust differences in average and regional FA values in schizophrenia patients, consistent with prior reports of patients with this disorder (Agartz, et al. 2001; Buchsbaum, et al. 2003; Kanaan, et al. 2009; Lagopoulos, et al. 2013; Whitford, et al. 2010), including unmedicated first-episode patients (Karlsgodt, et al. 2009; Reis Marques, et al. 2013) and adolescents at risk for psychosis (Karlsgodt, et al. 2012; Peters and Karlsgodt 2015). Findings of regional patient-control differences suggest that associative WM areas serving higher cognitive functioning, such as the genu of the corpus callosum that connects the left and right frontal lobes, show more consistent and greater deficits than motor and sensory tracts such the fibers in the external and internal capsule (Agartz, et al. 2001; Buchsbaum, et al. 2003; Whitford, et al. 2010). These associative WM fibers contain thinly myelinated multimodal fibers and typically have a prolonged maturation course followed by a steeper decline with age, known since the classical work of Flechsig (Flechsig 1901). The prolonged development of associative WM tracks may expose these areas to the primary or secondary risk factors of schizophrenia and make them susceptible to the schizophrenia pathology.

The relationship between heterochronicity and schizophrenia is likely to be the consequence of genetic risk factors for schizophrenia. For instance, a genotype-by-age interaction that affects axonal integrity, glial cell density and cellular aging may promote the development of schizophrenia and drive the relationship between diagnosis and FA deficits. One example is the genetic variations in the *TP53* gene that alter oligodendrocyte development and aging mechanisms (Molina, et al. 2011); this is already among the candidate genes for schizophrenia (Lung, et al. 2009; Ni, et al. 2005). Variations in this gene have been associated with deficits in FA values and reduced concentration of neurochemicals indexing glial and axonal health such as *N*-acetylaspartate in frontal WM (Molina, et al. 2011), and at the same time they are associated with increases in the risk for schizophrenia.

The evidence for accelerated decline in FA values with age in schizophrenia patients is consistently reported (Friedman, et al. 2008; Knochel, et al. 2012; Kochunov, et al. 2012a; Mori, et al. 2007; Wright, et al. 2014; Wright, et al. 2015). The findings of no accelerated aging are also reported but these studies were performed in smaller cohorts (N=20–50) where age-by-diagnosis interaction analysis is challenged by low statistical power (Jones, et al. 2006; Voineskos, et al. 2010) The accelerated aging of cerebral WM may also lead to decline in connectivity in the functional networks that support higher cognition (Sheffield, et al. 2015). We previously found that the onset of the accelerated decline in FA values in schizophrenia was correlated (r^2=0.36) with rates of the normal age-related decline in a smaller sample (Kochunov, et al. 2012a). Here, around 40–50% of the variance across the different WM fiber tracts was explained by rates of normal decline and maturation, extending the initial report to this much larger sample.

The finding of a positive correlation between the effect size of patient-control differences and the rate of FA development may appear counterintuitive as tracts that reach maturation earlier in life are expected to have faster rates of maturation. We used the rate of FA development reported from measurements in a large, cross-sectional sample of subjects aged 11–90 years (Kochunov, et al. 2012b). Here, WM tracts that reach peak FA values early in life will have lower rates of increasing FA during the measurement period, while those tracts that reach maturation in the 3rd and 4th decades may still undergo increased rates of change

(Figure 1). This may have led to a positive correlation between rate of FA development and the age of peak FA (Kochunov, et al. 2012b). Therefore, the regional variability in FA development is clearly an important empirical metric, but caution is needed in interpreting these trends.

The origin of the heterochronicity of WM development is not fully understood but is likely to be caused by regional differences in the rates of generating functionally mature oligodendrocytes and establishment of inter-neuronal communication that lead to myelination of active circuits (Gibson, et al. 2014). Microscopy studies showed that oligodendrocytes that myelinate the associative tracts connecting multimodal areas are morphologically distinct from those that myelinate primary motor and sensory tracts (Lamantia and Rakic 1990; Pfefferbaum, et al. 2000; Sullivan, et al. 2001; Wood P. and Bunger RP. 1984). The oligodendrocytes of the associative WM tracts also have slower rates of myelin repair (Hof, et al. 1990; Wakana, et al. 2004). Their myelination starts with a transient ensheathment of a large number of axons but only those axons that experience frequent electrical stimulation will remain myelinated (Hines, et al. 2015). Furthermore, engagement in higher cognitive and social functions requires sufficient myelination of associative WM tracts, but not for the tracts that serve the motor and sensory functions (Liu, et al. 2012; Makinodan, et al. 2012). Therefore, the prolonged development of multimodal associative fibers may stem from the need to support higher cognitive and social functions that emerge in adolescence and develop through middle adulthood, functions that are compromised in schizophrenia.

At present, DTI is the most commonly used neuroimaging technique to study diffusion properties of the brain. DTI is one of many diffusion weighted imaging (DWI) approaches and DTI-FA is a mathematic concepts derived for convenience rather than for biological interpretations(Basser and Pierpaoli 1996). Reduced FA values are commonly interpreted as an indexing reduced myelination, axonal damage or increased degree of intravoxel crossing based on findings in animal models and neurodegenerative disorder (Beaulieu 2002; Jones, et al. 2013; Song, et al. 2003; Song, et al. 2005). Reduced FA values in schizophrenia may be caused by several, complex factors. Advance DWI approaches such as diffusion kurtosis imaging (DKI) and multi-compartmental diffusion signal modeling have been used to clarify the neurobiology of FA differences in schizophrenia (Jensen and Helpern 2010; Kochunov, et al. 2014b; Zhu, et al. 2014) including the direct comparisons in a region with essentially no major crossing fiber architecture (sagittal band of corpus callosum)(Kochunov, et al. 2013; Kochunov, et al. 2014b; Zhu, et al. 2014). Reduced FA values in schizophrenia patients were associated with the rise in the free water component, reduction in permeability-diffusivity index and higher diffusion kurtosis values (Kochunov, et al. 2013; Zhu, et al. 2014). The findings were interpreted as potentially reduced myelin level or abnormalities in trans-membrane ion channels. This is consistent with reports of reduced axonal myelin levels and glial cells density by postmortem brain studies (Tkachev, et al. 2003; Uranova, et al. 2001; Uranova, et al. 2011; Uranova, et al. 2004) and findings from cellular neurobiology and genetic discovery studies (Blasius, et al. 2011; Freedman, et al. 2000; Huffaker, et al. 2009; Meyer, et al. 2001; Smolin, et al. 2011; Smoller, et al. 2013). Further analyses are needed to clarify the biological factors that underwrite the findings of reduced FA values in this disorder.

Our analyses took advantage of the novel ENIGMA-DTI mega-analytic data homogenization approach. Mega-analytic estimates of the effect of diagnosis on the regional FA values were in excellent (r>0.95) agreement with the classic meta-analytic estimates. Both mega-and-meta analytic estimates also showed good agreement with regional results derived from the individual cohorts (r=0.94, 0.84 and 0.71, for cohorts A, B and C, respective).

A potential limitation of this work is that the rates of the maturation and decline for different WM areas were derived based on cross-sectional rather than longitudinal measurements(Kochunov, et al. 2012b). We cannot rule out effects from chronic antipsychotic exposure in SCZ cohorts. The mega-analytic testing of anti-psychotic medication effects, as calculated by the correlation of CPZ on the whole-brain and regional FA, was not statistically significant (all p>0.3). This design does not allow differentiation of factors involved in schizophrenia etiology from effects of chronic antipsychotic medication exposure. Ascertainment of a large antipsychotic-naive SZ patient group is important, across different ages, to rule out interactions between medication effects and aging. Smoking is another possible contributing or confounding factor, because long-term smoking leads to decline in FA (Gons, et al. 2011; Kim, et al. 2010). Here, we observed no significant mega-analytical effect of smoking status on the whole-brain average FA values. Regionally, the mega-analytic effects of smoking (being a smoker vs a non-smoker) were nominally significant for the *corona radiata* tract (p=0.02) but this did not pass correction for multiple comparisons.

We note that this manuscript used age-of-peak values provided in (Kochunov, et al. 2012b), calculated using quadratic models. However, some have criticized this method in favor of spline fits of aging trends, as the variable age range can influence peak time estimates (Fjell, et al. 2010). The present work should not be adversely affected by these limitations for two reasons: First, we did not perform analyses in a sample with variable age range, so regional variations in age-of-peak cannot be attributed to range effects. Second, the correlations between effects of schizophrenia and accelerated aging with age-of-peak did not reach statistical significance.

In conclusion, our study is the largest schizophrenia DTI analysis to date. We found that tract-specific heterochronicity of normal WM development modulates the presentation of patient-control differences in WM FA values in schizophrenia. WM tracts that carry higher cognitive information and continue to mature past the average age-of-onset of schizophrenia are more sensitive to the pathophysiology of this disorder. The finding suggests the importance of implementing better white matter protection and treatment in supporting neurocognitive function and rehabilitation in individuals with this disorder. This study also posits regional WM measurements as promising endophenotypes for future studies of the genetic risks for schizophrenia.

Supplementary Material

Refer to Web version on PubMed Central for supplementary material.

Acknowledgments

Support was received from NIH grants U01MH108148, R01EB015611, R01DA027680, R01MH085646, P50MH103222, NSF IIS-1302755 and NSF MRI-1531491 and T32MH067533. This work was also supported in part by a Pfizer research grant and by the NIH Big Data to Knowledge (BD2K) Initiative (U54 EB020403).

References

Agartz I, Andersson JL, Skare S. Abnormal brain white matter in schizophrenia: a diffusion tensor imaging study. Neuroreport. 2001; 12(10):2251–4. [PubMed: 11447344]

Alba-Ferrara LM, de Erausquin GA. What does anisotropy measure? Insights from increased and decreased anisotropy in selective fiber tracts in schizophrenia. Front Integr Neurosci. 2013; 7:9. [PubMed: 23483798]

Bartzokis G. Age-related myelin breakdown: a developmental model of cognitive decline and Alzheimer's disease. Neurobiol Aging. 2004; 25(1):5–18. [PubMed: 14675724]

Bartzokis G, Cummings JL, Sultzer D, Henderson VW, Nuechterlein KH, Mintz J. White matter structural integrity in healthy aging adults and patients with Alzheimer disease: a magnetic resonance imaging study. Arch Neurol. 2003; 60(3):393–8. [PubMed: 12633151]

Bartzokis G, Lu PH, Tingus K, Mendez MF, Richard A, Peters DG, Oluwadara B, Barrall KA, Finn JP, Villablanca P, Thompson PM, Mintz J. Lifespan trajectory of myelin integrity and maximum motor speed. Neurobiology of aging. 2010; 31(9):1554–62. [PubMed: 18926601]

Basser PJ. Focal magnetic stimulation of an axon. IEEE Transactions on Biomedical Engineering. 1994; 41(6):601–6. [PubMed: 7927380]

Basser PJ, Pierpaoli C. Microstructural and physiological features of tissues elucidated by quantitative-diffusion-tensor MRI. J Magn Reson B. 1996; 111(3):209–19. [PubMed: 8661285]

Beaulieu C. The basis of anisotropic water diffusion in the nervous system - a technical review. NMR Biomed. 2002; 15(7–8):435–55. [PubMed: 12489094]

Ben Bashat D, Ben Sira L, Graif M, Pianka P, Hendler T, Cohen Y, Assaf Y. Normal white matter development from infancy to adulthood: comparing diffusion tensor and high b value diffusion weighted MR images. J Magn Reson Imaging. 2005; 21(5):503–11. [PubMed: 15834918]

Blasius AL, Dubin AE, Petrus MJ, Lim BK, Narezkina A, Criado JR, Wills DN, Xia Y, Moresco EM, Ehlers C, Knowlton KU, Patapoutian A, Beutler B. Hypermorphic mutation of the voltage-gated sodium channel encoding gene Scn10a causes a dramatic stimulus-dependent neurobehavioral phenotype. Proc Natl Acad Sci U S A. 2011; 108(48):19413–8. [PubMed: 22087007]

Bloemen OJ, de Koning MB, Schmitz N, Nieman DH, Becker HE, de Haan L, Dingemans P, Linszen DH, van Amelsvoort TA. White-matter markers for psychosis in a prospective ultra-high-risk cohort. Psychol Med. 2010; 40(8):1297–304. [PubMed: 19895720]

Brown S. Excess mortality of schizophrenia. A meta-analysis. Br J Psychiatry. 1997; 171:502–8. [PubMed: 9519087]

Buchsbaum MS, Shihabuddin L, Brickman AM, Miozzo R, Prikryl R, Shaw R, Davis K. Caudate and putamen volumes in good and poor outcome patients with schizophrenia. Schizophr Res. 2003; 64(1):53–62. [PubMed: 14511801]

Budde MD, Kim JH, Liang HF, Schmidt RE, Russell JH, Cross AH, Song SK. Toward accurate diagnosis of white matter pathology using diffusion tensor imaging. Magn Reson Med. 2007; 57(4):688–95. [PubMed: 17390365]

Carletti F, Woolley JB, Bhattacharyya S, Perez-Iglesias R, Fusar Poli P, Valmaggia L, Broome MR, Bramon E, Johns L, Giampietro V, Williams SC, Barker GJ, McGuire PK. Alterations in white matter evident before the onset of psychosis. Schizophr Bull. 2012; 38(6):1170–9. [PubMed: 22472474]

Conturo TE, McKinstry RC, Akbudak E, Robinson BH. Encoding of anisotropic diffusion with tetrahedral gradients: a general mathematical diffusion formalism and experimental results. Magn Reson Med. 1996; 35(3):399–412. [PubMed: 8699953]

Ellison-Wright I, Bullmore E. Meta-analysis of diffusion tensor imaging studies in schizophrenia. Schizophr Res. 2009; 108(1–3):3–10. [PubMed: 19128945]

Fjell AM, Walhovd KB, Westlye LT, Ostby Y, Tamnes CK, Jernigan TL, Gamst A, Dale AM. When does brain aging accelerate? Dangers of quadratic fits in cross-sectional studies. Neuroimage. 2010; 50(4):1376–83. [PubMed: 20109562]

Flechsig P. Developmental (myelogenetic) localisation of the cerebral cortex in the human. Lancet. 1901; 158:1027–30.

Freedman R, Adams CE, Leonard S. The alpha7-nicotinic acetylcholine receptor and the pathology of hippocampal interneurons in schizophrenia. J Chem Neuroanat. 2000; 20(3–4):299–306. [PubMed: 11207427]

Friedman JI, Tang C, Carpenter D, Buchsbaum M, Schmeidler J, Flanagan L, Golembo S, Kanellopoulou I, Ng J, Hof PR, Harvey PD, Tsopelas ND, Stewart D, Davis KL. Diffusion tensor imaging findings in first-episode and chronic schizophrenia patients. Am J Psychiatry. 2008; 165(8):1024–32. [PubMed: 18558643]

Gao W, Lin W, Chen Y, Gerig G, Smith JK, Jewells V, Gilmore JH. Temporal and spatial development of axonal maturation and myelination of white matter in the developing brain. AJNR Am J Neuroradiol. 2009; 30(2):290–6. [PubMed: 19001533]

Gibson EM, Purger D, Mount CW, Goldstein AK, Lin GL, Wood LS, Inema I, Miller SE, Bieri G, Zuchero JB, Barres BA, Woo PJ, Vogel H, Monje M. Neuronal activity promotes oligodendrogenesis and adaptive myelination in the mammalian brain. Science. 2014; 344(6183): 1252304. [PubMed: 24727982]

Glahn DC, Kent JW Jr, Sprooten E, Diego VP, Winkler AM, Curran JE, McKay DR, Knowles EE, Carless MA, Goring HH, Dyer TD, Olvera RL, Fox PT, Almasy L, Charlesworth J, Kochunov P, Duggirala R, Blangero J. Genetic basis of neurocognitive decline and reduced white-matter integrity in normal human brain aging. Proc Natl Acad Sci U S A. 2013; 110(47):19006–11. [PubMed: 24191011]

Gons RA, van Norden AG, de Laat KF, van Oudheusden LJ, van Uden IW, Zwiers MP, Norris DG, de Leeuw FE. Cigarette smoking is associated with reduced microstructural integrity of cerebral white matter. Brain. 2011; 134(Pt 7):2116–24. [PubMed: 21705426]

Hasan KM, Iftikhar A, Kamali A, Kramer LA, Ashtari M, Cirino PT, Papanicolaou AC, Fletcher JM, Ewing-Cobbs L. Development and aging of the healthy human brain uncinate fasciculus across the lifespan using diffusion tensor tractography. Brain Res. 2009a; 1276:67–76. [PubMed: 19393229]

Hasan KM, Kamali A, Iftikhar A, Kramer LA, Papanicolaou AC, Fletcher JM, Ewing-Cobbs L. Diffusion tensor tractography quantification of the human corpus callosum fiber pathways across the lifespan. Brain Res. 2009b; 1249:91–100. [PubMed: 18996095]

Hennekens CH, Hennekens AR, Hollar D, Casey DE. Schizophrenia and increased risks of cardiovascular disease. Am Heart J. 2005; 150(6):1115–21. [PubMed: 16338246]

Hines JH, Ravanelli AM, Schwindt R, Scott EK, Appel B. Neuronal activity biases axon selection for myelination in vivo. Nat Neurosci. 2015; 18(5):683–9. [PubMed: 25849987]

Hof PR, Cox K, Morrison JH. Quantitative analysis of a vulnerable subset of pyramidal neurons in Alzheimer's disease: I. Superior frontal and inferior temporal cortex. J Comp Neurol. 1990; 301(1):44–54. [PubMed: 2127598]

Huffaker SJ, Chen J, Nicodemus KK, Sambataro F, Yang F, Mattay V, Lipska BK, Hyde TM, Song J, Rujescu D, Giegling I, Mayilyan K, Proust MJ, Soghoyan A, Caforio G, Callicott JH, Bertolino A, Meyer-Lindenberg A, Chang J, Ji Y, Egan MF, Goldberg TE, Kleinman JE, Lu B, Weinberger DR. A primate-specific, brain isoform of KCNH2 affects cortical physiology, cognition, neuronal repolarization and risk of schizophrenia. Nat Med. 2009; 15(5):509–18. [PubMed: 19412172]

Ito K, Barnes PJ. COPD as a disease of accelerated lung aging. Chest. 2009; 135(1):173–80. [PubMed: 19136405]

Jahanshad N, Kochunov P, Sprooten E, Mandl RC, Nichols TE, Almassy L, Blangero J, Brouwer RM, Curran JE, de Zubicaray GI, Duggirala R, Fox PT, Hong LE, Landman BA, Martin NG, McMahon KL, Medland SE, Mitchell BD, Olvera RL, Peterson CP, Starr JM, Sussmann JE, Toga AW, Wardlaw JM, Wright MJ, Hulshoff Pol HE, Bastin ME, McIntosh AM, Deary IJ, Thompson PM, Glahn DC. Multi-site genetic analysis of diffusion images and voxelwise heritability analysis: A pilot project of the ENIGMA-DTI working group. NeuroImage. 2013a

Jahanshad N, Kochunov P, Sprooten E, Mandl RC, Nichols TE, Almassy L, Blangero J, Brouwer RM, Curran JE, de Zubicaray GI, Duggirala R, Fox PT, Hong LE, Landman BA, Martin NG, McMahon KL, Medland SE, Mitchell BD, Olvera RL, Peterson CP, Starr JM, Sussmann JE, Toga AW, Wardlaw JM, Wright MJ, Hulshoff Pol HE, Bastin ME, McIntosh AM, Deary IJ, Thompson PM, Glahn DC. Multi-site genetic analysis of diffusion images and voxelwise heritability analysis: A pilot project of the ENIGMA-DTI working group. Neuroimage. 2013b; pii: S1053-8119(13)00408-4. doi: 10.1016/j.neuroimage.2013.04.061

Jensen JH, Helpern JA. MRI quantification of non-Gaussian water diffusion by kurtosis analysis. NMR Biomed. 2010; 23(7):698–710. [PubMed: 20632416]

Jeste DV, Wolkowitz OM, Palmer BW. Divergent trajectories of physical, cognitive, and psychosocial aging in schizophrenia. Schizophr Bull. 2011; 37(3):451–5. [PubMed: 21505111]

Jones DK, Catani M, Pierpaoli C, Reeves SJ, Shergill SS, O'Sullivan M, Golesworthy P, McGuire P, Horsfield MA, Simmons A, Williams SC, Howard RJ. Age effects on diffusion tensor magnetic resonance imaging tractography measures of frontal cortex connections in schizophrenia. Hum Brain Mapp. 2006; 27(3):230–8. [PubMed: 16082656]

Jones DK, Knosche TR, Turner R. White matter integrity, fiber count, and other fallacies: the do's and don'ts of diffusion MRI. Neuroimage. 2013; 73:239–54. [PubMed: 22846632]

Kanaan R, Barker G, Brammer M, Giampietro V, Shergill S, Woolley J, Picchioni M, Toulopoulou T, McGuire P. White matter microstructure in schizophrenia: effects of disorder, duration and medication. Br J Psychiatry. 2009; 194(3):236–42. [PubMed: 19252154]

Karlsgodt KH, Jacobson SC, Seal M, Fusar-Poli P. The relationship of developmental changes in white matter to the onset of psychosis. Curr Pharm Des. 2012; 18(4):422–33. [PubMed: 22239573]

Karlsgodt KH, Niendam TA, Bearden CE, Cannon TD. White matter integrity and prediction of social and role functioning in subjects at ultra-high risk for psychosis. Biol Psychiatry. 2009; 66(6):562–9. [PubMed: 19423081]

Kim SH, Yun CH, Lee SY, Choi KH, Kim MB, Park HK. Age-dependent association between cigarette smoking on white matter hyperintensities. Neurol Sci. 2010; 33(1):45–51.

Kirkpatrick B, Messias E, Harvey PD, Fernandez-Egea E, Bowie CR. Is schizophrenia a syndrome of accelerated aging? Schizophr Bull. 2008; 34(6):1024–32. [PubMed: 18156637]

Knochel C, Oertel-Knochel V, Schonmeyer R, Rotarska-Jagiela A, van de Ven V, Prvulovic D, Haenschel C, Uhlhaas P, Pantel J, Hampel H, Linden DE. Interhemispheric hypoconnectivity in schizophrenia: fiber integrity and volume differences of the corpus callosum in patients and unaffected relatives. Neuroimage. 2012; 59(2):926–34. [PubMed: 21964509]

Kochunov P, Castro C, Davis D, Dudley D, Brewer J, Zhang Y, Kroenke CD, Purdy D, Fox PT, Simerly C, Schatten G. Mapping primary gyrogenesis during fetal development in primate brains: high-resolution in utero structural MRI of fetal brain development in pregnant baboons. Front Neurosci. 2010a; 4:20. [PubMed: 20631812]

Kochunov P, Chiappelli J, Hong LE. Permeability-diffusivity modeling vs. fractional anisotropy on white matter integrity assessment and application in schizophrenia. NeuroImage: Clinical. 2013; 3(0):18–26. [PubMed: 24179845]

Kochunov P, Chiappelli J, Wright S, Rowland L, Patel B, Wijtenburg S, Nugent K, McMahon R, Carpenter W, Muellerklein F, Sampath H, Hong L. Multimodal White Matter Imaging to Investigate Reduced Fractional Anisotropy and Its Age-Related Decline in Schizophrenia. Psychiatry Research: Neuroimaging. 2014a In Press.

Kochunov P, Chiappelli J, Wright SN, Rowland LM, Patel B, Wijtenburg SA, Nugent K, McMahon RP, Carpenter WT, Muellerklein F, Sampath H, Hong LE. Multimodal white matter imaging to investigate reduced fractional anisotropy and its age-related decline in schizophrenia. Psychiatry research. 2014b; 223(2):148–56. [PubMed: 24909602]

Kochunov P, Glahn D, Lancaster J, Winkler A, Kent J, Olvera R, Cole S, Dyer T, Almasy L, Duggirala R, Fox P, Blangero J. Whole Brain and Regional Hyperintense White Matter Volume and Blood Pressure: Overlap of Genetic Loci produced by Bivariate, Whole-Genome Linkage Analyses. Stroke. 2010b; 41(10):2137–42. [PubMed: 20724716]

Kochunov P, Glahn DC, LMR, Olvera R, Wincker P, Yang D, Sampath H, Carpenter W, Duggirala R, Curran J, Blangero J, Hong LE. Testing the hypothesis of accelerated cerebral white matter aging

in schizophrenia and major depression. Biol Psychiatry. 2012a; doi: 10.1016/j.biopsych.2012.10.002

Kochunov P, Glahn DC, Lancaster J, Thompson PM, Kochunov V, Rogers B, Fox P, Blangero J, Williamson DE. Fractional anisotropy of cerebral white matter and thickness of cortical gray matter across the lifespan. Neuroimage. 2011a; 58(1):41–9. [PubMed: 21640837]

Kochunov P, Glahn DC, Lancaster J, Winkler A, Karlsgodt K, Olvera RL, Curran JE, Carless MA, Dyer TD, Almasy L, Duggirala R, Fox PT, Blangero J. Blood pressure and cerebral white matter share common genetic factors in Mexican Americans. Hypertension. 2011b; 57(2):330–5. [PubMed: 21135356]

Kochunov P, Hong LE. Neurodevelopmental and neurodegenerative models of schizophrenia: white matter at the center stage. Schizophr Bull. 2014; 40(4):721–8. [PubMed: 24870447]

Kochunov P, Jahanshad N, Marcus D, Winkler A, Sprooten E, Nichols TE, Wright SN, Hong LE, Patel B, Behrens T, Jbabdi S, Andersson J, Lenglet C, Yacoub E, Moeller S, Auerbach E, Ugurbil K, Sotiropoulos SN, Brouwer RM, Landman B, Lemaitre H, den Braber A, Zwiers MP, Ritchie S, van Hulzen K, Almasy L, Curran J, deZubicaray GI, Duggirala R, Fox P, Martin NG, McMahon KL, Mitchell B, Olvera RL, Peterson C, Starr J, Sussmann J, Wardlaw J, Wright M, Boomsma DI, Kahn R, de Geus EJ, Williamson DE, Hariri A, van ‘t Ent D, Bastin ME, McIntosh A, Deary IJ, Hulshoff Pol HE, Blangero J, Thompson PM, Glahn DC, Van Essen DC. Heritability of fractional anisotropy in human white matter: A comparison of Human Connectome Project and ENIGMA-DTI data. Neuroimage. 2015a; 111:300–311. [PubMed: 25747917]

Kochunov P, Jahanshad N, Sprooten E, Nichols TE, Mandl RC, Almasy L, Booth T, Brouwer RM, Curran JE, de Zubicaray GI, Dimitrova R, Duggirala R, Fox PT, Elliot Hong L, Landman BA, Lemaitre H, Lopez LM, Martin NG, McMahon KL, Mitchell BD, Olvera RL, Peterson CP, Starr JM, Sussmann JE, Toga AW, Wardlaw JM, Wright MJ, Wright SN, Bastin ME, McIntosh AM, Boomsma DI, Kahn RS, den Braber A, de Geus EJ, Deary IJ, Hulshoff Pol HE, Williamson DE, Blangero J, van ‘t Ent D, Thompson PM, Glahn DC. Multi-site study of additive genetic effects on fractional anisotropy of cerebral white matter: Comparing meta and megaanalytical approaches for data pooling. Neuroimage. 2014c; 95C:136–150.

Kochunov P, Thompson PM, Winkler A, Morrissey M, Fu M, Coyle TR, Du X, Muellerklein F, Savransky A, Gaudiot C, Sampath H, Eskandar G, Jahanshad N, Patel B, Rowland L, Nichols TE, O’Connell JR, Shuldiner AR, Mitchell BD, Hong LE. The common genetic influence over processing speed and white matter microstructure: Evidence from the Old Order Amish and Human Connectome Projects. Neuroimage. 2015b; 125:189–197. [PubMed: 26499807]

Kochunov P, Williamson DE, Lancaster J, Fox P, Cornell J, Blangero J, Glahn DC. Fractional anisotropy of water diffusion in cerebral white matter across the lifespan. Neurobiol Aging. 2012b; 33(1):9–20. [PubMed: 20122755]

Kubicki M, McCarley R, Westin CF, Park HJ, Maier S, Kikinis R, Jolesz FA, Shenton ME. A review of diffusion tensor imaging studies in schizophrenia. J Psychiatr Res. 2007; 41(1–2):15–30. [PubMed: 16023676]

Lagopoulos J, Hermens DF, Hatton SN, Battisti RA, Tobias-Webb J, White D, Naismith SL, Scott EM, Ryder WJ, Bennett MR, Hickie IB. Microstructural white matter changes are correlated with the stage of psychiatric illness. Transl Psychiatry. 2013; 3:e248. [PubMed: 23612047]

Lamantia AS, Rakic P. Cytological and quantitative characteristics of four cerebral commissures in the rhesus monkey. J Comp Neurol. 1990; 291(4):520–37. [PubMed: 2329189]

Liu J, Dietz K, DeLoyht JM, Pedre X, Kelkar D, Kaur J, Vialou V, Lobo MK, Dietz DM, Nestler EJ, Dupree J, Casaccia P. Impaired adult myelination in the prefrontal cortex of socially isolated mice. Nat Neurosci. 2012; 15(12):1621–3. [PubMed: 23143512]

Lung FW, Shu BC, Kao WT, Chen CN, Ku YC, Tzeng DS. Association of DRD4 uVNTR and TP53 codon 72 polymorphisms with schizophrenia: a case-control study. BMC Med Genet. 2009; 10:147. [PubMed: 20040103]

Madler B, Drabycz SA, Kolind SH, Whittall KP, MacKay AL. Is diffusion anisotropy an accurate monitor of myelination? Correlation of multicomponent T2 relaxation and diffusion tensor anisotropy in human brain. Magn Reson Imaging. 2008; 26(7):874–88. [PubMed: 18524521]

Makinodan M, Rosen KM, Ito S, Corfas G. A critical period for social experience-dependent oligodendrocyte maturation and myelination. Science. 2012; 337(6100):1357–60. [PubMed: 22984073]

Meyer J, Huberth A, Ortega G, Syagailo YV, Jatzke S, Mossner R, Strom TM, Ulzheimer-Teuber I, Stober G, Schmitt A, Lesch KP. A missense mutation in a novel gene encoding a putative cation channel is associated with catatonic schizophrenia in a large pedigree. Mol Psychiatry. 2001; 6(3): 302–6. [PubMed: 11326298]

Molina V, Papiol S, Sanz J, Rosa A, Arias B, Fatjo-Vilas M, Calama J, Hernandez AI, Becker J, Fananas L. Convergent evidence of the contribution of TP53 genetic variation (Pro72Arg) to metabolic activity and white matter volume in the frontal lobe in schizophrenia patients. Neuroimage. 2011; 56(1):45–51. [PubMed: 21296169]

Mori T, Ohnishi T, Hashimoto R, Nemoto K, Moriguchi Y, Noguchi H, Nakabayashi T, Hori H, Harada S, Saitoh O, Matsuda H, Kunugi H. Progressive changes of white matter integrity in schizophrenia revealed by diffusion tensor imaging. Psychiatry Res. 2007; 154(2):133–45. [PubMed: 17276660]

Nazeri A, Mallar Chakravarty M, Felsky D, Lobaugh NJ, Rajji TK, Mulsant BH, Voineskos AN. Alterations of Superficial White Matter in Schizophrenia and Relationship to Cognitive Performance. Neuropsychopharmacology. 2012

Ni X, Trakalo J, Valente J, Azevedo MH, Pato MT, Pato CN, Kennedy JL. Human p53 tumor suppressor gene (TP53) and schizophrenia: case-control and family studies. Neurosci Lett. 2005; 388(3):173–8. [PubMed: 16039051]

Perez-Iglesias R, Tordesillas-Gutierrez D, McGuire PK, Barker GJ, Roiz-Santianez R, Mata I, de Lucas EM, Rodriguez-Sanchez JM, Ayesa-Arriola R, Vazquez-Barquero JL, Crespo-Facorro B. White matter integrity and cognitive impairment in first-episode psychosis. Am J Psychiatry. 2011; 167(4):451–8.

Peters BD, Karlsgodt KH. White matter development in the early stages of psychosis. Schizophr Res. 2015; 161(1):61–9. [PubMed: 24893908]

Pfefferbaum A, Sullivan EV, Hedehus M, Lim KO, Adalsteinsson E, Moseley M. Age-related decline in brain white matter anisotropy measured with spatially corrected echo-planar diffusion tensor imaging. Magn Reson Med. 2000; 44(2):259–68. [PubMed: 10918325]

Phillips KA, Rogers J, Barrett EA, Glahn DC, Kochunov P. Genetic contributions to the midsagittal area of the corpus callosum. Twin Res Hum Genet. 2012; 15(3):315–23. [PubMed: 22856367]

Pierpaoli C, Basser PJ. Toward a quantitative assessment of diffusion anisotropy. Magn Reson Med. 1996; 36(6):893–906. [PubMed: 8946355]

R-Development-Core-Team. R: A Language and Environment for Statistical Computing. 2009.

Reis Marques T, Taylor H, Chaddock C, Dell'acqua F, Handley R, Reinders AA, Mondelli V, Bonaccorso S, Diforti M, Simmons A, David AS, Murray RM, Pariante CM, Kapur S, Dazzan P. White matter integrity as a predictor of response to treatment in first episode psychosis. Brain. 2013

Saha S, Chant D, McGrath J. A systematic review of mortality in schizophrenia: is the differential mortality gap worsening over time? Arch Gen Psychiatry. 2007; 64(10):1123–31. [PubMed: 17909124]

Sheffield JM, Repovs G, Harms MP, Carter CS, Gold JM, MacDonald AW 3rd, Ragland JD, Silverstein SM, Godwin D, Barch DM. Evidence for Accelerated Decline of Functional Brain Network Efficiency in Schizophrenia. Schizophr Bull. 2015

Smith SM, Jenkinson M, Johansen-Berg H, Rueckert D, Nichols TE, Mackay CE, Watkins KE, Ciccarelli O, Cader MZ, Matthews PM, Behrens TE. Tract-based spatial statistics: voxelwise analysis of multi-subject diffusion data. Neuroimage. 2006; 31(4):1487–505. [PubMed: 16624579]

Smolin B, Karry R, Gal-Ben-Ari S, Ben-Shachar D. Differential expression of genes encoding neuronal ion-channel subunits in major depression, bipolar disorder and schizophrenia: implications for pathophysiology. Int J Neuropsychopharmacol. 2011; 15(7):869–82. [PubMed: 22008100]

Smoller JW, Craddock N, Kendler K, Lee PH, Neale BM, Nurnberger JI, Ripke S, Santangelo S, Sullivan PF. Identification of risk loci with shared effects on five major psychiatric disorders: a genome-wide analysis. Lancet. 2013; 381(9875):1371–9. [PubMed: 23453885]

Song SK, Sun SW, Ju WK, Lin SJ, Cross AH, Neufeld AH. Diffusion tensor imaging detects and differentiates axon and myelin degeneration in mouse optic nerve after retinal ischemia. Neuroimage. 2003; 20(3):1714–22. [PubMed: 14642481]

Song SK, Yoshino J, Le TQ, Lin SJ, Sun SW, Cross AH, Armstrong RC. Demyelination increases radial diffusivity in corpus callosum of mouse brain. Neuroimage. 2005; 26(1):132–40. [PubMed: 15862213]

Sullivan EV, Adalsteinsson E, Hedehus M, Ju C, Moseley M, Lim KO, Pfefferbaum A. Equivalent disruption of regional white matter microstructure in ageing healthy men and women. Neuroreport. 2001; 12(1):99–104. [PubMed: 11201100]

Tkachev D, Mimmack ML, Ryan MM, Wayland M, Freeman T, Jones PB, Starkey M, Webster MJ, Yolken RH, Bahn S. Oligodendrocyte dysfunction in schizophrenia and bipolar disorder. Lancet. 2003; 362(9386):798–805. [PubMed: 13678875]

Tsuang MT, Woolson RF. Excess mortality in schizophrenia and affective disorders. Do suicides and accidental deaths solely account for this excess? Arch Gen Psychiatry. 1978; 35(10):1181–5. [PubMed: 697536]

Ulug AM, Barker PB, van Zijl PC. Correction of motional artifacts in diffusion-weighted images using a reference phase map. Magn Reson Med. 1995; 34(3):476–80. [PubMed: 7500889]

Uranova N, Orlovskaya D, Vikhreva O, Zimina I, Kolomeets N, Vostrikov V, Rachmanova V. Electron microscopy of oligodendroglia in severe mental illness. Brain Res Bull. 2001; 55(5):597–610. [PubMed: 11576756]

Uranova NA, Vikhreva OV, Rachmanova VI, Orlovskaya DD. Ultrastructural alterations of myelinated fibers and oligodendrocytes in the prefrontal cortex in schizophrenia: a postmortem morphometric study. Schizophr Res Treatment. 2011; 2011:325789. [PubMed: 22937264]

Uranova NA, Vostrikov VM, Orlovskaya DD, Rachmanova VI. Oligodendroglial density in the prefrontal cortex in schizophrenia and mood disorders: a study from the Stanley Neuropathology Consortium. Schizophr Res. 2004; 67(2–3):269–75. [PubMed: 14984887]

van Erp TG, Hibar DP, Rasmussen JM, Glahn DC, Pearlson GD, Andreassen OA, Agartz I, Westlye LT, Haukvik UK, Dale AM, Melle I, Hartberg CB, Gruber O, Kraemer B, Zilles D, Donohoe G, Kelly S, McDonald C, Morris DW, Cannon DM, Corvin A, Machielsen MW, Koenders L, de Haan L, Veltman DJ, Satterthwaite TD, Wolf DH, Gur RC, Gur RE, Potkin SG, Mathalon DH, Mueller BA, Preda A, Macciardi F, Ehrlich S, Walton E, Hass J, Calhoun VD, Bockholt HJ, Sponheim SR, Shoemaker JM, van Haren NE, Pol HE, Ophoff RA, Kahn RS, Roiz-Santianez R, Crespo-Facorro B, Wang L, Alpert KI, Jonsson EG, Dimitrova R, Bois C, Whalley HC, McIntosh AM, Lawrie SM, Hashimoto R, Thompson PM, Turner JA. Subcortical brain volume abnormalities in 2028 individuals with schizophrenia and 2540 healthy controls via the ENIGMA consortium. Mol Psychiatry. 2015

Voineskos AN, Lobaugh NJ, Bouix S, Rajji TK, Miranda D, Kennedy JL, Mulsant BH, Pollock BG, Shenton ME. Diffusion tensor tractography findings in schizophrenia across the adult lifespan. Brain. 2010; 133(Pt 5):1494–504. [PubMed: 20237131]

Wakana S, Jiang H, Nagae-Poetscher LM, van Zijl PC, Mori S. Fiber tract-based atlas of human white matter anatomy. Radiology. 2004; 230(1):77–87. [PubMed: 14645885]

Wheeler AL, Voineskos AN. A review of structural neuroimaging in schizophrenia: from connectivity to connectomics. Front Hum Neurosci. 2014; 8:653. [PubMed: 25202257]

Whitford TJ, Kubicki M, Schneiderman JS, O'Donnell LJ, King R, Alvarado JL, Khan U, Markant D, Nestor PG, Niznikiewicz M, McCarley RW, Westin CF, Shenton ME. Corpus callosum abnormalities and their association with psychotic symptoms in patients with schizophrenia. Biol Psychiatry. 2010; 68(1):70–7. [PubMed: 20494336]

Wood, P.; Bunger, RP. The biology of the oligodendrocyte. In: WTN, editor. Oligodendroglia. New York: Plenum Press; 1984. p. 1-46.

Wright S, Kochunov P, Chiappelli J, McMahon R, Muellerklein F, Wijtenburg SA, White MG, Rowland L, Hong E. Accelerated White Matter Aging in Schizophrenia: Role of White Matter Blood Perfusion. Neurobiol Aging. 2014; In Press. doi: 10.1016/j.neurobiolaging.2014.02.016

Wright SN, Hong LE, Winkler AM, Chiappelli J, Nugent K, Muellerklein F, Du X, Rowland LM, Wang DJ, Kochunov P. Perfusion shift from white to gray matter may account for processing speed deficits in schizophrenia. Hum Brain Mapp. 2015

Yakovlev, PI.; Lecours, A-R. The myelogenetic cycles of regional maturation of the brain. In: Minkowski, A., editor. Regional development of the brain in early life. Oxford: Blackwell Scientific Publications; 1967. p. 3-65.

Yendiki A, Koldewyn K, Kakunoori S, Kanwisher N, Fischl B. Spurious group differences due to head motion in a diffusion MRI study. Neuroimage. 2014; 88C:79–90.

Zhu J, Zhuo C, Qin W, Wang D, Ma X, Zhou Y, Yu C. Performances of diffusion kurtosis imaging and diffusion tensor imaging in detecting white matter abnormality in schizophrenia. Neuroimage Clin. 2014; 7:170–6. [PubMed: 25610778]

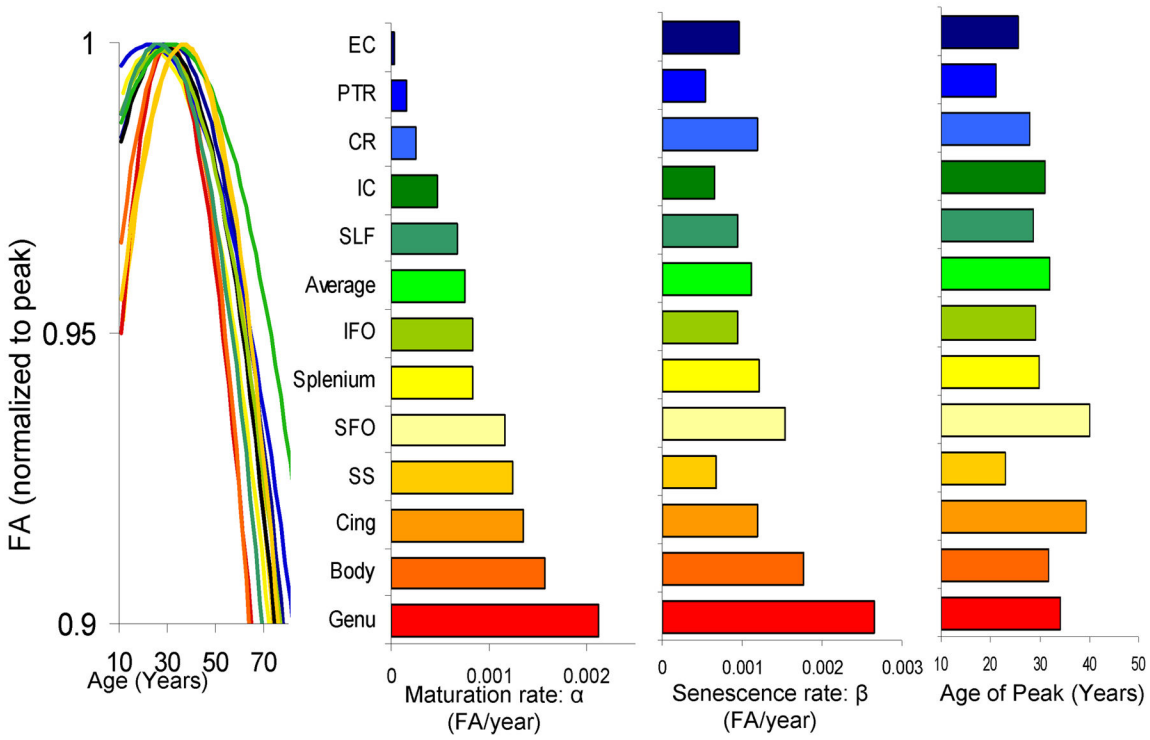

Figure 1.

Regional heterochronicity of white matter development color-coded based on the rate of normal maturation during adolescence (*top row*). These measurements were derived using FA extracted from a large (N=831) cross-sectional sample of normal subjects (age range=11–90 years) and presented in (Kochunov, et al. 2012b).

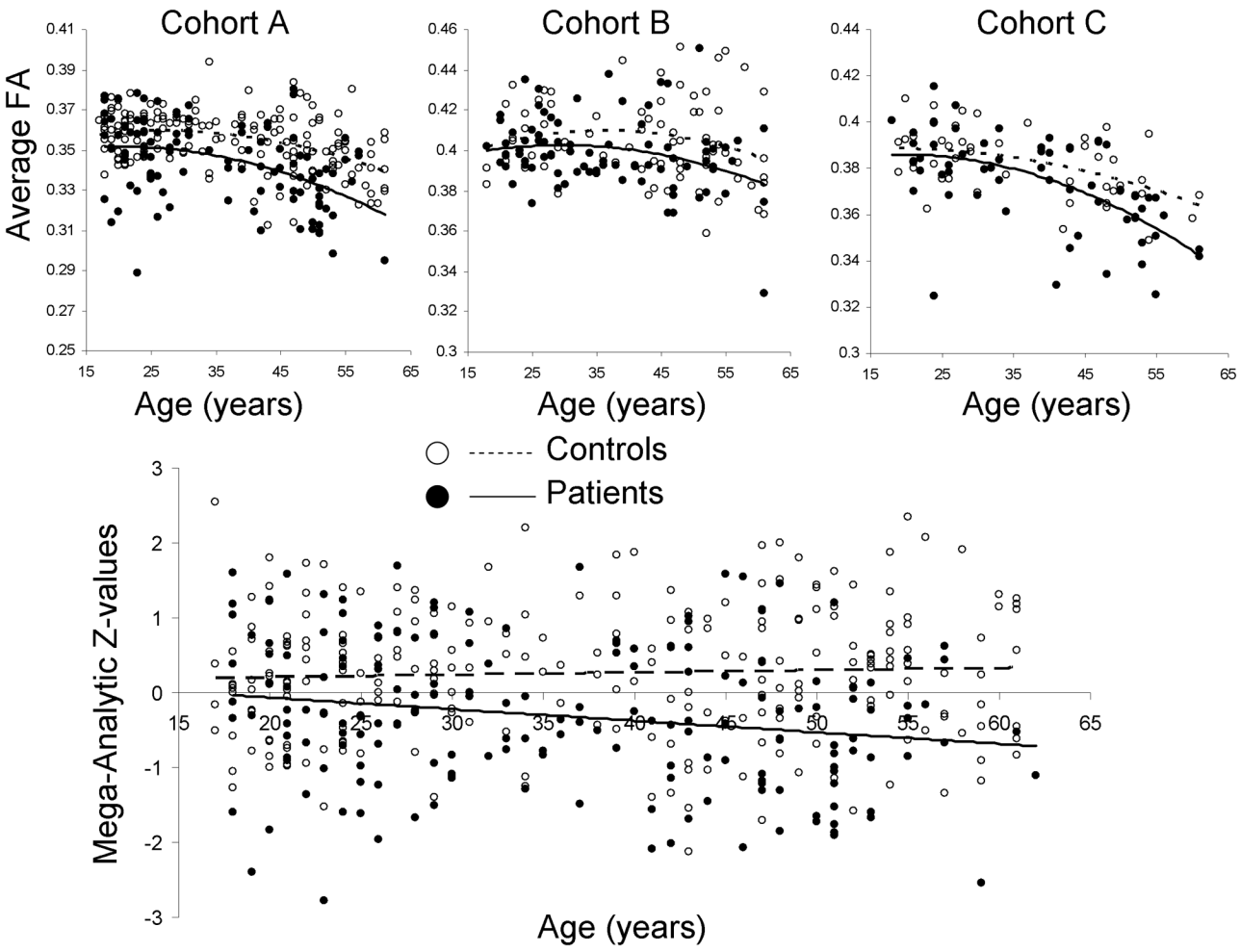

Figure 2.

Mega-analytic analysis of the effects of diagnosis (DX) and DX by age interaction. The non-linear aging trends in FA values are regressed in each cohort separately, thus producing linear trends of patient-control differences in aging.

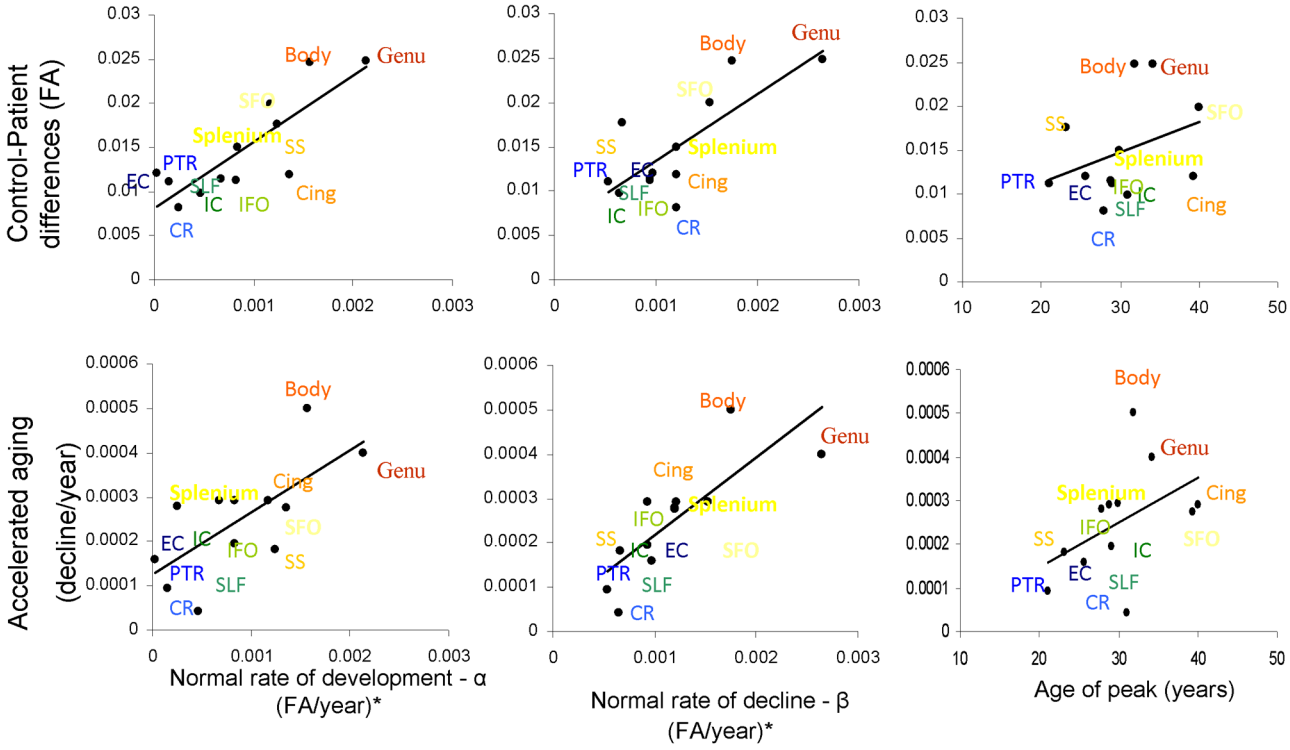

Figure 3.

Mega-analytic estimates of patient control differences (*top row*) and accelerated aging (*bottom row*) are plotted versus the rates of normal development and decline and age of peak for FA values derived from a large cohort (N=831) of normal subjects aged 11–90 years (Kochunov, et al. 2012b).

Table 1

White matter tracts used in the analysis (C=Commissural, P=Projection, A=Association). The rates of normal age-related maturation, age-of-peak and the rate of age-related decline were taken from (Kochunov, et al. 2012b).

Area	Fiber Type	Connections	Rate of maturation (*10^{-4} FA/year)	Rate of senescence (*10^{-4} FA/year)	Age of peak (years)
Average FA values			7.5	11.7	32.1
Genu of Corpus Callosum (GCC)	C/A	Cerebral Hemispheres	21.3	26.5	34.2
Body of Corpus Callosum (BCC)	C/A	Cerebral Hemispheres	14.7	17.6	31.8
Splenium of Corpus Callosum (SCC)	C/A	Cerebral Hemispheres	8.4	12.1	29.9
Cingulum (Cing)	A	Cingulate Gyrus/Hippocampus	13.6	12.0	39.4
Corona Radiata (CR)	P	Cortical/Subcortical	2.5	12.0	27.9
External Capsule (EC)	A	Frontal/Temporal/Occipital	0.3	9.7	25.6
Internal Capsule (IC)	P	Subcortical/Brainstem/Cortex	10.9	14.5	31.0
Superior Frontal-Occipital (SFO)	A	Frontal/Parietal/Occipital	11.7	15.3	40.1
Inferior Frontal Occipital (IFO)	A	Frontal/Parietal/Occipital	8.3	9.4	29.1
Posterior Thalamic Radiation (PTR)	P	Thalamus/Cortex	1.5	5.4	28.8
Sagittal Stratum (SS)	A/P	Occipital/Temporal	12.4	6.7	23.1
Superior Longitudinal Fasciculus (SLF)	A	Frontal/Temporal/Occipital	6.8	9.4	28.8

Table 2

Subject demographics for three cohorts. The severity of psychiatric symptoms was ascertained using Brief Psychiatric Rating Scale (BPRS). Medical dose is provided in chlorpromazine equivalent dose (mg/day). The severity of tobacco dependence was ascertained using the Fagerstrom Test for Nicotine Dependence (FTDN). Processing speed measurements were performed using digit symbol substitution task (DSST). IQ data was only collected in Cohort A.

		Average Age, Range (years)	BPRS	Age-of-Onset (years)	Illness Duration (years)	Education (year)	IQ	Handedness (% right)	Medication Dose (CPZ)	Current Smokers	FTND	DSST Processing Speed
Cohort A	Patients (44M/21F)	34.6±13.7 18–61	30.7±11.0	18.1±8.5	21.5±15.1	13.0±2.0	91.1±15.5	90.2	400.5±352.2	29%	4.2±2.1	55.2±15.7
	Controls (61M/79F)	35.6±14.4 18–61	n/a	n/a	n/a	14.0±2.5	97.8±18.5	98.0	n/a	27%	4.1±2.1	73.5±15.6
	p value	0.6	n/a	n/a	n/a	0.003	0.06	0.15	n/a	0.9	0.3	10^{-10}
Cohort B	Patients (61M/62F)	35.3±9.5 20–61	30.7±9.5	18.9±7.8	20.1±13.7	13.0±2.2	n/c	83.0	630.5±544.2	55%	5.1±2.3	47.3±11.3
	Controls (31M/45F)	40.3±11.9 20–61	n/a	n/a	n/a	14.5±2.5	n/c	88.3	n/a	35%	5.3±2.2	64.9±11.6
	p value	0.006	n/a	n/a	n/a	0.001	n/c	0.43	n/a	0.15	0.1	10^{-9}
Cohort C	Patients (50M/13F)	37.7±12.5 18–61	31.2±8.5	18.5±7.5	19.7±13.6	12.2±2.2	n/c	87.8	453.5±371.6	68%	4.7±2.5	51.6±14.9
	Controls (27M/18F)	39.1±13.8 20–61	n/a	n/a	n/a	14.9±2.5	n/c	88.1	n/a	44%	4.5±2.6	68.9±14.6
	p value	0.60	n/a	n/a	n/a	0.001	n/c	0.83	n/a	0.01	0.5	10^{-7}

Table 3

The β_{DX} ± standard errors are shown, following multiplication by ($-1*10^2$) factor, with the corresponding p-values for the whole-brain and regional analysis of impact of diagnosis on white matter FA values. The β_{DX} values indicate (Control – Patient)/100 difference, in FA values. Bolded values are significant after correcting for multiple (N=12) comparisons. Nominally significant values are shown in *italic*

	Cohort A	Cohort B	Cohort C	Mega	Meta
Average	**1.21±0.21 (p=3.0E-08)**	**0.91±0.31 (p=4E-03)**	**0.85±0.35 (p=6E-03)**	**1.1±0.1 (p=1E-11)**	**p=2E-10**
Genu of Corpus Callosum (GCC)	**2.8±0.50 (p=1.0E-07)**	*2.74±0.91 (p=8E-03)*	**2.2±0.88 (p=3E-03)**	**2.5±0.4 (p=1E-10)**	**p=8E-10**
Body of Corpus Callosum (BCC)	**3.81±0.71 (p=1E-07)**	2.5±0.80 (p=0.06)	*1.6±1.2 (p=4E-03)*	**2.4±0.5 (p=8.0E-08)**	**p=1E-07**
Splenium of Corpus Callosum (SCC)	**2.24±0.40 (p=9E-08)**	1.02±1.05 (p=0.3)	0.65±0.8 (p=0.15)	**1.50±0.3 (p=4E-06)**	**p=7E-05**
Cingulum (Cing)	**1.50±0.43 (p=4E-05)**	0.50±0.70 (p=0.2)	1.45±0.81 (p=0.1)	**1.2±0.3 (p=1E-05)**	**p=8E-05**
Corona Radiata (CR)	**1.70±0.40 (p=9E-11)**	*1.4±0.7 (p=0.01)*	*0.45±0.30 (p=0.03)*	**1.5±0.2 (p=3E-11)**	**p=3E-10**
Internal Capsule (IC)	**2.51±0.43 (p=2E-09)**	*1.94±0.68 (p=0.04)*	**1.2±0.50 (p=2E-03)**	**0.9±0.2 (p=1E-5)**	**p=2.0E-5**
External Capsule (EC)	**1.50±0.35 (p=1E-06)**	1.41±0.44 (p=0.05)	**0.90±0.45 (p=2.5E-03)**	**1.2±0.2 (p=2E-9)**	**p=2E-08**
Superior Frontal-Occipital (SFO)	**2.2±0.45 (p=3E-07)**	**1.8±0.65 (p=3E-04)**	*2.40±0.60 (p=0.01)*	**2.0±0.3 (p=8E-11)**	**p=1E-9**
Inferior Frontal Occipital (IFO)	**1.51±0.51 (p=4E-03)**	0.21±0.81 (p=0.15)	1.00±0.75 (p=0.5)	**1.0±0.40 (p=3E-03)**	*p=0.008*
Posterior Thalamic Radiation (PTR)	**1.48±0.45 (p=2.5E-04)**	0.5±0.60 (p=0.07)	2.2±0.87 (p=0.1)	**1.1±0.2 (p=1E-05)**	**p=7E-05**
Sagittal Stratum (SS)	**2.1±0.39 (p=6E-08)**	*1.62±0.65 (p=0.04)*	*1.3±0.57 (p=0.01)*	**1.7±0.3 (p=4E-10)**	**p=1E-9**
Superior Longitudinal Fasciculus (SLF)	**1.45±0.35 (p=3E-05)**	*1.35±0.50 (p=0.05)*	*1.40±0.6 (p=0.01)*	**1.1±0.2 (p=7E-07)**	**p=1E-06**

Table 4

The β_{Age*DX} ± standard error (p-values) are shown, after multiplication by -10^4 scaling factor, for whole-brain and regional analysis of accelerated (FA units/year) decline with in patients (DX=1). Higher, positive β_{Age*DX} values indicate greater decline with age. Bolded values are significant after correcting for multiple (N=12) comparisons. Nominally significant values are shown in *italic.*

	Cohort A	**Cohort B**	**Cohort C**	**Mega**	**Meta**
Average	**1.60±0.8 (p=0.04)**	1.23±1.40 (p=0.3)	**1.45±1.15 (p=0.04)**	**1.22±0.63 (p=0.02)**	**p=0.04**
Genu of Corpus Callosum (GCC)	**5.4±1.9 (p=4.0E-03)**	*7.2±3.8 (p=0.05)*	4.10±3.5 (p=0.09)	***4.4±1.5 (p=0.004)***	***p=0.01***
Body of Corpus Callosum (BCC)	**12.3±2.5 (p=5.0E-05)**	*8.4±3.6 (p=0.01)*	0.5±3.9 (p=0.5)	**5.0±2.0 (p=1.0E-04)**	**p=1E-03**
Splenium of Corpus Callosum (SCC)	*3.38±1.5 (p=0.01)*	*7.6±4.0 (p=0.03)*	*4.93±2.97 (p=0.05)*	*2.9±1.3 (p=0.01)*	*p=0.03*
Cingulum (Cing)	**3.6±1.7 (p=1E-03)**	**5.1±2.6 (p=1E-03)**	−0.19±2.61 (p=0.5)	*2.7±1.25 (p=0.02)*	*p=0.02*
Corona Radiata (CR)	**3.8±1.2 (p=1E-03)**	*2.1±1.5 (p=0.01)*	*3.20±1.96 (p=0.04)*	**2.7±0.92 (p=1.0E-03)**	**p=2.0E-03**
Internal Capsule (IC)	*3.3±1.20 (p=8.0E-03)*	3.5±2.1 (p=0.07)	1.12±1.67 (p=0.3)	0.4±0.9 (p=0.4)	p=0.05
External Capsule (EC)	**2.5±1.1 (p=1E-03)**	1.2±1.8 (p=0.28)	0.21±1.73 (p=0.45)	*1.6±0.81 (p=0.04)*	p=0.07
Superior Frontal-Occipital (SFO)	*2.1±1.2 (p=0.01)*	2.6±2.6 (p=0.2)	2.06±2.51 (p=0.21)	*2.9±1.2 (p=0.01)*	*p=0.02*
Inferior Frontal Occipital (IFO)	**5.1±2.3 (p=1.3E-03)**	−3.0±3.5 (p=0.8)	0.60±3.12 (p=0.42)	1.9± 1.6(p=0.1)	p=0.2
Posterior Thalamic Radiation (PTR)	0.4±1.2 (p=0.4)	1.1±2.4 (p=0.3)	*7.43±3.30 (p=0.01)*	0.9±1.37 (p=0.2)	p=0.2
Sagittal Stratum (SS)	1.07±1.5 (p=0.4)	1.7±2.5 (p=0.2)	*5.03±2.11 (p=0.01)*	*1.8±1.1 (p=0.05)*	*p=0.1*
Superior Longitudinal Fasciculus (SLF)	1.2±1.3 (p=0.3)	0.6±1.8 (p=0.6)	*3.99±1.97 (p=0.02)*	*1.2±0.89 (p=0.1)*	p=0.15